Threshold switching via electric field induced crystallization in phase-change memory devices

Jorge A. Vázquez Diosdado, Peter Ashwin, Krisztian I. Kohary, and C. David Wright

Related Articles

Additional information on Appl. Phys. Lett.

Threshold switching via electric field induced crystallization in phase-change memory devices

Jorge A. Vázquez Diosdado, Peter Ashwin, Krisztian I. Kohary, and C. David Wright
College of Engineering, Mathematics and Physical Sciences, University of Exeter, Exeter EX4 4QF, United Kingdom

Phase-change devices exhibit characteristic threshold switching from the reset (off) to the set (on) state. Mainstream understanding of this electrical switching phenomenon is that it is initiated electronically via the influence of high electric fields on inter-band trap states in the amorphous phase. However, recent work has suggested that field induced (crystal) nucleation could instead be responsible. We compare and contrast these alternative switching "theories" via realistic simulations of device switching both with and without electric field dependent contributions to the system free energy. Results show that although threshold switching can indeed be obtained purely by electric field induced nucleation, the fields required are significantly larger than experimentally measured values. © 2012 American Institute of Physics. [http://dx.doi.org/10.1063/1.4729551]

Electrical phase change memories (PCMs) are of much topical interest as a potential next-generation non-volatile memory technology[1,2] and for possible advanced applications in such areas as arithmetic and neuromorphic processing.[3,4] PCMs utilize a reversible switching transition from a high-resistance (amorphous) state to low-resistance (crystalline) state in order to store data. A characteristic feature of the electrically driven amorphous to crystalline (SET) transition is the existence of a threshold electric field that must be exceeded for switching to occur. Mainstream understanding of this switching phenomenon is that it is initiated electronically via the influence of high electric fields on the inter-band trap states.[5–7] However, recent work has suggested that field induced (crystal) nucleation could instead be responsible,[7–12] and models for such field-induced nucleation were able to explain several experimental observations on PCM devices, such as the occurrence of relaxation oscillations[8,9] and the relationship between switching voltage (and temperature) and switching delay time.[10] Most models of field-induced nucleation presented to date have concentrated on the role of the electric field in lowering the nucleation barrier and the associated critical nucleus size, an approach extended recently by ourselves to include a fuller kinetic treatment that can identify field ranges where electric field effects might play a significant role in the crystallization of "bulk" samples.[13] However, the inclusion of possible field-induced nucleation effects in physically realistic models of electrical switching in actual PCM devices has so far been lacking. Therefore, in this letter, we investigate the SET (amorphous to crystal) transition in phase-change "mushroom" type cells both with and without electric field-induced nucleation effects; by this approach, we hope to determine whether or not field-induced nucleation is indeed the driving force behind the characteristic threshold switching behavior of PCMs.

To model the PCM switching process, we combine electrical, thermal, and phase-transformation models. The electrical and thermal models are implemented using finite-element software (COMSOL^TM) and solve, simultaneously, the Laplace and heat-diffusion equations. In the conventional approach to electrical modeling of PCMs, the experimentally observed threshold switching effect is usually described by some form of field-dependent electrical conductivity for the amorphous phase.[1,5,6,13,14] However, if threshold switching is really a result of field induced nucleation rather than a field-dependent conductivity of the amorphous phase, then an appropriate modeling approach is to include electric field energy terms in the crystallization model while excluding field-dependent conductivity from the electrical model; we use just such an approach below and compare the results to those obtained from a more conventional switching model.

Our phase-transformation model uses a Gillespie cellular automata (GCA) approach that combines thermodynamic features of rate-equation approaches[15] with elements from probabilistic cellular automata (PCA) models[16,17] and phase-field models;[18,19] in addition, it uses the Gillespie algorithm[20] for efficient time-stepping. Our GCA model has been previously described in detail[21] and in summary considers a homogeneous, isotropic material in a square lattice where the state of the material is described through a set of points in the lattice that can be either crystalline or amorphous. The state of each point (i,j) in the lattice is described by two quantities; r_{ij}, the phase of the (i,j) site (which takes the values 0 and 1 for amorphous and crystalline, respectively), and Φ_{ij} which defines an orientation (with two adjacent crystalline sites belonging to same crystallite (crystal grain) if they have the same orientation). The local changes that can occur are defined by three events: *nucleation,* where site (i,j) and an adjacent site, originally both amorphous, become a single crystallite; *growth,* where site (i,j), originally amorphous, becomes attached to an adjacent crystal; *dissociation,* where site (i,j), originally crystalline, detaches from the crystal of which it is a part to become amorphous. The rate at which each of these three events occur is determined by the system energy, which is usually described in terms of the Gibbs free energy G, where $G = (A\sigma - Vg)$ and A and V are the surface area and volume, respectively, of a crystal cluster, σ is the surface energy, and g is the bulk free energy difference

between phases. Traditionally (i.e., in most theoretical treatments of crystallization in phase-change materials and devices[2,5,14]), the bulk energy difference term g is considered to be purely temperature dependent (for example, as $g(T) = H_f$ $(7T/T_m)[(T_m - T)/(T_m + 6T)]$ where H_f is the enthalpy of fusion and T_m is the melting point[15]). However, as pointed out in recent works,[7–12] the formation of a (relatively) high-conductivity crystal nucleus in an otherwise (relatively) non-conducting amorphous matrix will decrease the electrostatic energy of the system. This additional energy term is incorporated into our GCA simulator by adding an electric field term to the bulk free energy difference g such that it is now a function of both temperature and electric field, i.e., $g(T,E) = g(T) + g(E)$ where $g(E) = 0.5E^2 \varepsilon / n$ and ε ($= \varepsilon_0 \varepsilon_r$) is the permittivity, and n is the depolarizing factor.[13] The rate $R(T,E)$ at which a site (i,j) transforms from amorphous to crystalline is thus given by[21]

$$R(T,E) = \nu . \exp\left(-\frac{\xi_a}{kT}\right)\exp\left(\frac{L(T_m - T)}{T} - \frac{\sigma A}{2kT} + \frac{\varepsilon E^2 V_m}{2nkT}\right),$$
(1)

where ξ_a is the activation energy, V_m is the volume of a basic unit (monomer) of the crystalline phase (for example, in $Ge_2Sb_2Te_5$, this is estimated[15] to be 2.9×10^{-22} cm^3), k is Boltzmann's constant, υ is a frequency factor, and $L = H_f$ $V_m / 2kT_m$. Equation (1) together with the algorithmic steps for the GCA simulator described previously[21] thus enable realistic simulation of phase-transitions in phase-change materials and devices, including the role of any electric field induced nucleation effects.

Before we turn our attention to PCM devices, we first investigate the role that electric field induced nucleation might play in the crystallization of "bulk" phase-change material. We consider the commonly used $Ge_2Sb_2Te_5$ alloy and evaluate the time taken for a sample of such material to completely crystallize under the influence of various (constant and uniform) temperatures and electric fields. Results are shown in Fig. 1(a) for the case of an 80 nm × 80 nm sample area and for the parameter values (taken from the literature1[13–15]) of $\xi_a = 2.0$ eV, $H_f = 1121$ Jcm^{-3}, $\sigma = 0.066$ Jm^{-2}, $\varepsilon = 100$, $T_m = 889$ K, and $\upsilon = 4 \times 10^{22}$ Hz. Figure 1 shows that at (relatively) low field values (<100 MVm^{-1}), the overall crystallization time at any particular temperature is relatively unaffected by the presence of the field, but at larger fields (>100 MVm^{-1}), there can be a reduction in crystallization time. For example, the sample crystallizes in $\sim$31 ns at a temperature of $\sim$405 °C for E lying between 1 MVm^{-1} and 100 MVm^{-1}, but for E $\approx$ 300 MVm^{-1}, a reduced temperature of 385 °C yields the same crystallization time. Note that the crystallization temperatures here are much higher than those reported from standard calorimetry (DSC) measurements of $Ge_2Sb_2Te_5$ (e.g., 155 °C in Ref. 22), but that recent ultra-fast DSC measurements[23] have shown that the crystallization temperature increases dramatically with heating rate (e.g., from $\sim$180 °C at 50 Ks^{-1} to $\sim$350 °C at 40 000 Ks^{-1}).

The results of Fig. 1(a) are of a similar form to those from a previous work in which only nucleation effects were considered.[13] The GCA approach however enables a more
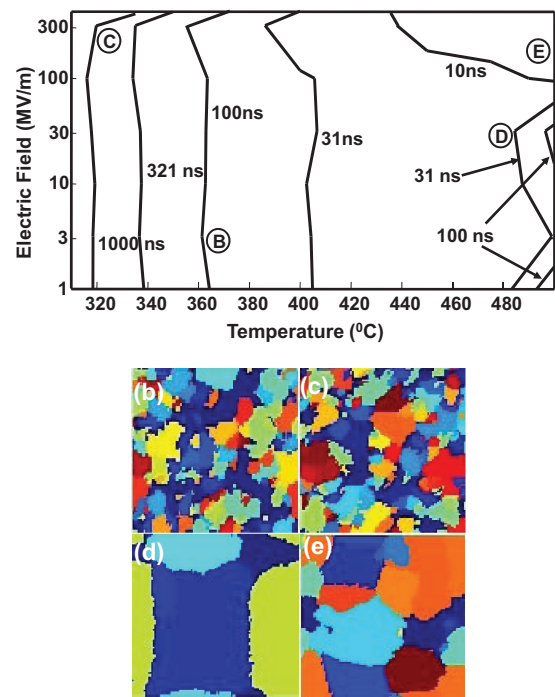

FIG. 1. (a) (top) Crystallization times and (b) to (e) crystal structures (each 80 nm × 80 nm) for $Ge_2Sb_2Te_5$ as a function of both temperature and electric field. The positions on the map in (a) to which the structures (b) to (e) relate are marked by the letters B, C, D, and E, respectively.

physically realistic simulation of nucleation *and* growth effects; moreover, by identifying the dominant crystallization mechanism in various regions of the (T,E) crystallization "map" of Fig. 1(a), we gain additional information on the likely role of field induced nucleation. For example, at all temperatures below $\sim$420 °C in Fig. 1, we found that crystallization proceeds primarily by nucleation, as typified by the crystal structure shown in Figs. 1(b) and 1(c); this behavior is consistent with the usual description of $Ge_2Sb_2Te_5$ as a "nucleation-dominant" material.[24,25] On the other hand, temperatures above $\sim$480 °C, when coupled with fields less than around 100 MVm^{-1}, lead to growth-dominated crystallization, as typified by the structure shown in Fig. 1(d) and consistent with recent experimental results showing that the growth velocity of $Ge_2Sb_2Te_5$ at relatively high temperatures is high.[23,26] Interestingly however, at high temperatures and high fields (>100 MVm^{-1}), the crystallization behavior again becomes more influenced by nucleation, as shown in Fig. 1(e), indicating that the electric field induced nucleation is playing a significant role in this region.

We now turn our attention to the study of electric field effects in a typical PCM device, specifically one with the "mushroom" cell structure shown in Fig. 2, with the aim of ascertaining whether or not field induced nucleation alone can account for the characteristic threshold switching. As outlined above, we use COMSOL^{TM} finite-element software for the (2D cylindrically symmetric) electro-thermal simulations, while crystallization is modeled using our own GCA code linked to (called from) COMSOL^{TM}. The GCA uses a rectangular mesh with square elements of size $\sim$0.82 nm (corresponding to the diameter of a "monomer" or "molecule" of $Ge_2Sb_2Te_5$—see Ref. 15 for more details). The time step for the GCA simulations is determined by the Gillespie

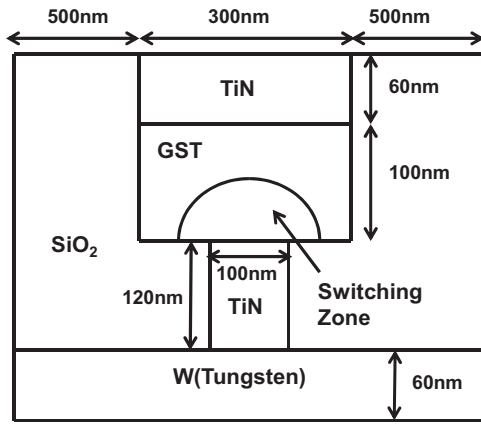FIG. 2. Schematic of the PCM "mushroom" cell used for the device simulations.

TABLE I. Material parameters.

	K (W/mK)	C (J/m^{3}K)	σ (Ωm)$^{-1}$
TiN (heater)	17	7×10^5	1.12×10^5
TiN (electrode)	19	2.16×10^6	5×10^6
SiO$_2$	1.4	3.1×10^6	1×10^{-16}
W (electrode)	175	2.35×10^6	18×10^6
Ge$_2$Sb$_2$Te$_5$ (amorph)	0.2	1.25×10^6	$\sigma_{0am}.\exp(\Delta\xi_{am}/KT)$[a]
Ge$_2$Sb$_2$Te$_5$ (crystal)	0.5	1.25×10^6	$\sigma_{0crys}.\exp(\Delta\xi_{crys}/KT)$[a]

[a]See Ref. 14.

algorithm, whereas for the electro-thermal simulations, the time step was 0.5 ns (chosen to ensure proper simulation of heating and cooling rates while giving reasonable computational times). The crystallization behavior and the electrical response of the PCM cell were investigated (compared) using three different approaches. Method I implements the conventional understanding of phase-change switching behavior, i.e., the amorphous phase conductivity is electric-field dependent, here as described by Ielmini and Zhang in Ref. 6, but the electric field *does not* contribute to the bulk free energy difference term, i.e., $g = g(T)$. Method II adds to this conventional approach the field energy term in the free energy, i.e., $g = g(T,E)$ to allow for the reduction of system energy by the formation of (relatively) high conducting crystal nuclei in an insulating (amorphous) matrix. Method III removes from the switching simulation any effects of the electric field on the conductivity of the amorphous phase but does allow for field induced crystallization; if such field induced crystallization is indeed the driving force for threshold switching in phase-change devices, then we should expect to see the characteristic threshold-type I-V curves for simulations using method III.

The results of I-V simulations for the PCM device of Fig. 2 are shown in Figs. 3(a) and 3(b); in all cases, a 30 ns/30 ns ramped up/down excitation voltage was used and a
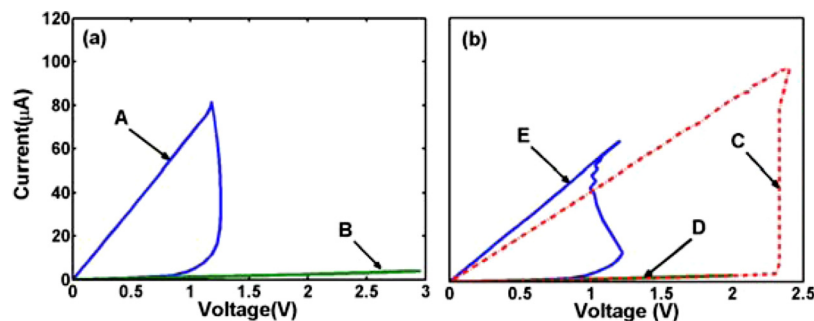
10 kΩ resistor was placed in series with the PCM cell (and the material parameters used in the simulations are given in Table I). Curve A in Fig. 3(a) is the I–V curve obtained using a "conventional" simulation approach, i.e., assuming the amorphous phase conductivity is electric field dependent but that the electric field does not contribute to the free energy (Method I); as expected, characteristic threshold switching is observed with the threshold voltage being around 1 V, in line with published experimental results for this type of device.[5,6,27] Also shown in Fig. 3(a) is the I–V curve obtained when the field dependent conductivity has been removed from the simulation (curve B); here no switching is evident even for relatively high applied voltages (3 V case shown, but no switching was observed even when the maximum voltage applied was increased to 4 V). Fig. 3(b) shows the I–V curves obtained when including the field dependent term in the free energy. Curve C in Fig. 3(b) is obtained by method III (i.e., the amorphous phase conductivity is not field dependent, but the field does contribute to the free energy); threshold switching is again evident but requires a significantly increased voltage (>2.5 V); indeed, smaller voltages than this produce no evidence of switching (as shown in case D). Also shown for completeness in Fig. 3(b) is the I–V curve (E) simulated using method II, i.e., assuming both a field dependent conductivity *and* a field term in the free energy. From these I–V curves, it would seem that both a field dependent conductivity (of the amorphous phase) and a field dependent term in the free energy are capable of generating the characteristic threshold switching, either operating separately (as in curves A and C) or in tandem (curve E). However, the voltages and fields required to induce

FIG. 3. Simulated I–V curves for the PCM device of Fig. 2. Curve A in (a) is the I–V curve obtained by method I (i.e., amorphous phase conductivity is electric field dependent but the electric field does not contribute to the free energy); note that threshold switching occurs at just over 1 V, in line with published experimental results (e.g., see Refs. 5 and 6). Also shown in (a) is case B for which the field dependent conductivity has been removed from the simulation and no switching is evident even for high applied voltages. Case C in (b) is the I–V curve obtained by method III (i.e., the amorphous phase conductivity is not field dependent, but the field does contribute to the free energy); threshold switching is again evident but requires a significantly increased voltage (>2.5 V); indeed, smaller voltages than this produce no evidence of switching (see curve D). Also shown (curve E) for completeness is the I–V curve simulated using method II (i.e., field dependent conductivity *and* field term in free energy).
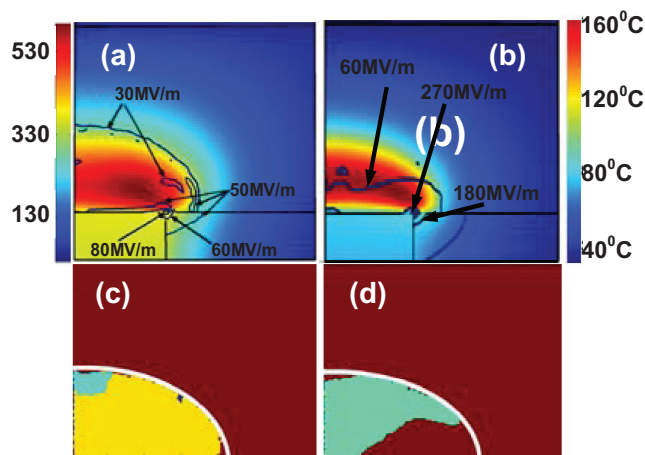
FIG. 4. Simulated device temperatures and electric fields ((a) and (b)) during the SET pulse at the time of the maximum field (i.e., at 22 ns for (a) and 26 ns for (b)) and crystallization structure ((c) and (d)) at the end of the SET pulse (the white contour shows the spatial extent of the starting amorphous dome and different colors correspond to different crystallite orientations). Figures (a) and (c) were obtained using method I (i.e., switching is electronically driven as described in Ref. 6), whereas (b) and (d) were obtained using method III (i.e., switching is driven by field-induced nucleation). The SET pulse was rectangular and of 60 ns duration in all cases, but the pulse amplitude in (b) and (d) was higher than in (a) and (c) (2.6 V and 2 V, respectively). Movies of the switching/crystallization process with and without the electric field energy included in the Gibbs free energy (enhanced online) [URL: http://dx.doi.org/10.1063/1.4729551.1] [URL: http://dx.doi.org/10.1063/1.4729551.2].

switching when we only include field dependent free energy in the simulations are large. This is exemplified in Fig. 4, where we compare the simulated temperature and fields in the "active" region of the PCM cell, and the final recrystallized structure, for simulations using method I (Figs. 4(a) and 4(c)) and method III (Figs. 4(b) and 4(d)). Movies of the entire switching/crystallization process for the case of Figs. 4(c) and 4(d) corresponding to switching driven by purely electronic processes (field-dependent amorphous phase conductivity) and purely field-induced nucleation are given in the supplementary multimedia information.

With a field dependent term in the free energy, but no field dependent conductivity, the fields required to induce switching are huge ($\sim$300 MVm^{-1}, see Fig. 4(b)) whereas with field dependent conductivity (and no field dependent free energy term), the threshold fields are much more reasonable ($\sim$60 MVm^{-1}) and in line with those measured experimentally.[28] We also note that varying any of the relevant parameters in (1) within what is thought to be a reasonable range did not result in a significant reduction in the threshold field for the field induced nucleation case.

In conclusion, physically realistic simulations of the SET (i.e., crystallization) process in electrical phase-change (Ge$_2$Sb$_2$Te$_5$) memory devices have shown that the threshold switching characteristic of such devices can be obtained by a mechanism driven purely by electric field induced nucleation, as recently suggested.[7–12] However, the fields necessary for such threshold switching by field induced nucleation alone are relatively high, being of the order 300 MVm^{-1}.

This is significantly larger than experimentally measured threshold fields[28] of around 56 MVm^{-1} (though we note that such experimental measurements are for lateral cells rather than the "mushroom" type cell considered here, and that threshold fields in other types of device such as the recently reported "interfacial" phase-change memory[29] may well be different). The threshold fields and switching voltages predicted using the more conventional explanation of threshold switching, i.e., electronic processes leading to a field-dependent amorphous phase conductivity, are much closer to those measured experimentally.

[1]H.-S. P. Wong, S. Raoux, S. Kim, J. Liang, J. P. Reifenberg, B. Rajendran, M. Asheghi, and K. E. Goodson, Proc. IEEE **98**, 2201 (2010).
[2]D. Lencer, M. Salinga, and M. Wuttig, Adv. Mater. **23**, 2030 (2010).
[3]C. D. Wright, Y. Liu, K. I. Kohary, M. M. Aziz, and R. J. Hicken, Adv. Mater. **23**, 3408 (2011).
[4]D. Kuzum, R. G. D. Jeyasingh, B. Lee, and H.-S. P. Wong, Nano Lett. **12**, 2179 (2012).
[5]A. Redaelli, A. Pirovano, A. Benvenuti, and A. L. Lacaita, J. Appl. Phys. **103**, 111101 (2008).
[6]D. Ielmini and Y. Zhang, J. Appl. Phys. **102**, 054517 (2007).
[7]M. Simon, M. Nardone, S. Kostylev, I. Karpov, and V. Karpov, in *Phase Change Materials for Memory and Reconfigurable Electronics, Symposium H, MRS Symposia Proceedings No. 1251* (Materials Research Society, Pittsburgh, 2010), p. H01.
[8]M. Nardone, V. G. Karpov, D. C. S. Jackson, and I. V. Karpov, Appl. Phys. Lett. **94**, 103509 (2009).
[9]M. Nardone, I. V. Karpov, and V. G. Karpov, J. Appl. Phys. **107**, 054519 (2010).
[10]I. V. Karpov, M. Mitra, D. Kau, G. Spandini, Y. A. Kryukov, and V. G. Karpov, Appl. Phys. Lett. **92**, 173501 (2008).
[11]V. G. Karpov, M. Nardone, and M. Simon, J. Appl. Phys. **109**, 114507 (2011).
[12]V. G. Karpov, Y. A. Kryukov, S. D. Savransky, and I. V. Karpov, Appl. Phys. Lett. **90**, 123504 (2007).
[13]K. I. Kohary and C. D. Wright, Appl. Phys. Lett. **98**, 223102 (2011).
[14]C. D. Wright, L. Wang, P. Shah, M. M. Aziz, E. Varesi, R. Bez, M. Moroni, and F. Cazzaniga, IEEE Trans. Nanotechnol. **10**, 900 (2011).
[15]S. Senkader and C. D. Wright, J. Appl. Phys. **95**, 504 (2004).
[16]W. Yu, C. D. Wright, S. P. Banks, and E. P. Palmiere, IEEE Proc.: Sci., Meas. Technol. **150**, 211 (2003).
[17]Y. Cao, D. T. Gillespie, and L. Petzold, J. Chem. Phys. **126**, 224101 (2007).
[18]S. Vedantam and B. S. V. Patnaik, Phys. Rev. E **73**, 016703 (2006).
[19]K. B. Blyuss, P. Ashwin, C. D. Wright, and A. P. Bassom, Physica D **215**, 127 (2006)
[20]D. T. Gillespie, J. Phys. Chem. **81**, 2340 (1977).
[21]P. Ashwin, B. S. V. Patnaik, and C. D. Wright, J. Appl. Phys. **104**, 084101 (2008).
[22]J. Kalb, F. Spaepen, and M. Wuttig, J. Appl. Phys. **93**, 2389 (2003).
[23]J. Orava, A. L. Greer, B. Gholipour, D. W. Hewak, and C. E. Smith, Nature Mater **11**, 279 (2012).
[24]M. Wuttig and N. Yamada, Nature Mater. **6**, 824 (2007).
[25]S. Raoux and M. Wuttig, *Phase Change Materials: Science and Applications* (Springer, 2008).
[26]K. F. Kelton and A. L. Greer, *Nucleation in Condensed Matter: Applications in Materials and Biology* (Pergamon Materials Series, 2010).
[27]A. L. Lacaita, A. Redaelli, D. Ielmini, F. Pellizzer, A. Pirovano, A. Benvenuti, and R. Bez, Tech. Dig. – Int. Electron Devices Meet. **2004**, 911.
[28]D. Krebs, S. Raoux, C. T. Rettner, G. W. Burr, M. Salinga, and M. Wuttig, Appl. Phys. Lett. **95**, 082101 (2009).
[29]R. E. Simpson, P. Fons, A. V. Kolobov, T. Fukaya, M. Krbal, T. Yagi, and J. Tominaga, Nat. Nanotechnol. **6**, 501 (2011).